JOURNAL OF MATERIALS SCIENCE 27 (1992) 4818–4827

Characterization of water-in-oil emulsions by means of dielectric spectroscopy

R. M. HILL
The Dielectrics Group, Department of Physics, King's College London, The Strand, London WC2R 2LS, UK

J. COOPER
ICI Explosives, Group Technical Centre, Ardeer Site, Stevenston, Ayrshire KA20 3LN, UK

A simple microscopic model of an array of water droplets separated by thin oil films is analysed and compared with experimental data from a range of water-in-oil emulsions of high volume fraction in order to delineate the nature of the cooperative effects in such systems. It is shown that a simple summation in series and parallel of the response of isolated particles is fundamentally incapable of giving an acceptable description of the experimental data as is the more complex theoretical model proposed by Hanai. The nature of the corrections to the model are considered from an experimental viewpoint, and the need for a model which is capable of reproducing all the aspects of the experimental situation is discussed.

1. Introduction

Dielectric spectroscopy is a convenient technique for the non-invasive examination of heterogeneous systems such as emulsions and gels [1–4]. The essence of the technique is that the electrical response is measured as a function of the frequency of an applied a.c. voltage and can be represented in any one of a number of equivalent forms, i.e. impedance, capacitance, admittance or modulus. In a typical heterogeneous system the flow of charge is impeded by barriers and this gives rise to local polarizations and hence dispersions in the response. If the components of the system are themselves dipolar, as is water, then there are further dispersions which may be identified as belonging to the individual components. The ease with which the technique can be applied has stimulated interest over a number of years and two reviews have been published by Clausse [2] and van Beek [5]. The problem is that conventional development of Maxwell's equations allows accurate description of dilute dispersions of particles in a medium but are not applicable to the more useful case of high packing fractions. Hanai [6, 7] has proposed a cooperative model for such systems which is unfortunately based on weak assumptions and which has not been shown to be of general applicability. Recently, a full cooperative relaxation model has been developed [8, 9] and has been shown to be applicable to gels [3, 4, 10]. It is our intention to show that this model is applicable to high phase volume emulsions, but before doing so we require to characterize the response of typical emulsions. This we do here.

We start by examining the characteristic response of a typical stable water-in-oil emulsion. To do so we consider a pair of particles and the oil/emulsion film between them. A single particle can be characterized by the capacitance and conductance of the liquid that it contains. A pair of particles requires that we place in series with the first particle a barrier layer which can also be characterized by its capacitance and conductance. With a thin oil–emulsifier barrier and a water-based particle it is reasonable to assume that the barrier conductance will be less than that of the particle conductance and the capacitance of the barrier greater than that of the particle. Hence the physical basis of the conventional approach to heterogeneous systems is an electrical model of a pair of parallel connected conductance and capacitance elements connected in series. From this element the complete structure may be modelled by connecting similar elements in parallel across the electrode plates and stacking these in series through the thickness of the sample.

Here we consider this simple approach and compare it with good experimental data in order to show where its defects lie and how these may be corrected. To do so we make use of the cluster model of relaxation [8, 9] which is based on the cooperative relaxation of a volume distribution of dynamically interactive particles and hence is ideally suited for application to emulsion systems.

One experimental difficulty that is encountered is the extraordinarily wide range of relaxation times present in water-oil-emulsion systems. Four such relaxation times are of significance; the relaxation time for the dipoles forming the liquid within the particles, which may be typically of the order of nanoseconds; the relaxation time for the transport of charge across a single emulsion particle, which may be of the order of microseconds; the relaxation time of charges separated by a single oil–emulsifier barrier layer which we estimate to be of the order of kiloseconds and the relaxation time of the bulk macroscopic sample which

0022–2461

can be of the order of tens of seconds. The seconds to nano-second range emphasizes the need for extensive high-quality experimental data. Without this it is not possible to determine, with any certainty, which process is which and hence to make full use of the information that is available. The technique of data normalization [11, 12] is effective in this situation and recourse will be made to this helpful method of analysis when necessary.

2. Theory

The problem of high phase volume dispersions has been considered by Lissant [13] who has proposed two regular plane-surfaced structures as possible candidates for the form of the particles. These are the tetrakaidecahedron (a truncated octahedron) and the rhomboidal dodecahedron. It was suggested that incomplete packing is achieved by the rounding off of the vertices of these space-filling structures. Consideration by Lissant of a geometrical factor, the ratio of the surface area of a particle to the two-thirds root of its volume, has shown that between 68% and 74% internal phase the tetrakaidecahedron structure would be possible but would be likely to break up into spherical particles of a range of sizes. Between 74% and about 94% internal phase, the rhomboidal dodecahedron packing would be preferred, whereas above 94%, the tetrakaidecahedron would be geometrically preferred and physically stable.

One difficulty of either of these regular structures is that because of the multi-faceting it is not possible to determine either an effective cross-sectional area or an effective barrier thickness for the boundary layers between the particles along a specific direction. We do know, however, that for a uniform filling of particles the boundaries must traverse the complete area of the electrodes and hence we take this area, A, as the effective area and denote the effective thickness of a single barrier, normal to the electrode plane, as d_b. We do not expect d_b to be identical to the length of the hydrocarbon chain of the emulsifier but we accept that the thickness of the films between the droplets is likely to be independent of the dispersed phase volume fraction and a function of both the surfactant chain length and of the forces across the thickness of the film. However, we do expect d_b to change in magnitude if the physical structure or phase of the system were to change.

Consider a cell with plane parallel electrodes of area A and separation D filled with particles of a regular shape of size L. If the capacitance of each particle is C_p, the effective geometrical capacitance of the three dimensional array is

$$\begin{aligned} C_{eff} &= C_p(A/L^2)(L/D) \\ &= C_p(A/LD) \end{aligned} \quad (1)$$

But C_p is itself given by

$$C_p = \varepsilon_p \varepsilon_0 (a/d) \quad (2)$$

where ε_0 is the permittivity of free space (8.854×10^{-12} F m^{-1}), ε_p the relative permittivity of the material forming the particle and a and d are the effective area and length of the particle. We relate these to the particle size by setting

$$\begin{aligned} \frac{a}{d} &= \gamma \frac{L^2}{L} \\ &= \gamma L \end{aligned} \quad (3)$$

where γ ($\leqslant 1$) is an undetermined structure factor. Hence we have

$$C_{eff} = \varepsilon_p \varepsilon_0 \gamma \frac{A}{D} \quad (4)$$

and, as the empty cell capacitance, C_0, is given by $\varepsilon_0(A/D)$

$$\begin{aligned} \varepsilon_{eff} &= \varepsilon_p \gamma \\ &= C_{eff}/C_0 \end{aligned} \quad (5)$$

defines the effective permittivity of the liquid within the particles without knowledge of the structure factor, γ. It is clear, from Equation 3, that γ will take its maximum value of unity for a system of tightly packed regular cubes with their faces parallel to the electrode plane. As suggested for the effective particle spacing, we expect γ to be sensitive to the structure of the array of the particles and note that through γ we have related the microscopic permittivity, ε_p, to the macroscopic value, ε_{eff}.

A similar approach can be developed for the conductance of the array, G_{eff}. If the conductivity of the liquid within the particle is σ_p, then we have

$$G_{eff}/C_0 = \sigma_p \gamma/\varepsilon_0 \quad (6)$$

The relaxation time which can be associated with the measured capacitance and conductance, C_{eff} and G_{eff}, is then given by

$$\begin{aligned} \tau_1 &= C_{eff}/G_{eff} \\ &= \varepsilon_0 \varepsilon_{eff}/\sigma_p \\ &= \tau_p \end{aligned} \quad (7)$$

where τ_p is the relaxation time of the material within the particles. Hence the observation of the macroscopic capacitance and conductance yields information about the microscopic system.

We use the term "relaxation time" in its general form which is given by the definition

$$\begin{aligned} \tau &= RC \\ &= \sigma \frac{d}{A} \varepsilon \varepsilon_0 \frac{A}{d} \\ &= \varepsilon \varepsilon_0 / \sigma \end{aligned} \quad (8)$$

where the symbols have their conventional meanings. Recasting this equation into the form of a complex capacitance

$$C(\omega) = C'(\omega) - iC''(\omega) \quad (9)$$

and defining ω_c as the frequency for which

$$\begin{aligned} C'(\omega_c) &= G/\omega_c \\ &= C''(\omega_c) \end{aligned} \quad (10)$$

we have that each crossing of the real and imaginary components of the complex capacitance (impedance,

admittance or modulus) in a dispersion diagram defines a relaxation time for the system with $\tau_n = (\omega_{c,n})^{-1}$.

We now assume that the barriers between the particles are of the same area, a, as that of the particles so that the actual barrier capacitance is given by

$$C_b = \varepsilon_0 \varepsilon_b \beta (a/d_b) \quad (11)$$

where β is a second barrier structure factor. ε_b, the relative permittivity of the barrier material, is likely to be small for the non-polar hydrocarbon chains involved. We relate this capacitance to the cell size as

$$\begin{aligned} C_{b(\text{eff})} &= C_b \frac{A}{L^2} \frac{L}{d} \\ &= \varepsilon_0 \varepsilon_b \frac{a}{d_b} \beta \frac{A}{Ld} \\ &= \varepsilon_0 \varepsilon_b \gamma \beta \frac{A}{d_b} \end{aligned} \quad (12)$$

The conductance of the barrier is given by

$$G_b = \sigma_b \beta (A/d_b) \quad (13)$$

so that the relaxation time associated with a single barrier is

$$\begin{aligned} \tau_2 &= \varepsilon_0 \varepsilon_b \frac{A}{d_b} \frac{d_b}{\sigma_b A} \\ &= \varepsilon_0 \varepsilon_b / \sigma_b \\ &= \tau_b \end{aligned} \quad (14)$$

In both Equations 7 and 14 the resistance and capacitance elements taking part in the relaxation are in parallel and hence the areas and thicknesses cancel out so that the macroscopic relaxation times give direct measures of the microscopic values. We note, too, that these values will be independent of the size of the particles and therefore independent of any distribution of sizes that may exist.

This is not the case when the charges associated with transport within the particles are blocked by the capacitance of the barriers. In this case the Maxwell–Wagner [5, 12] relaxation time for the series resistance–capacitance combination is given by

$$\begin{aligned} \tau_3 &= \varepsilon_0 \varepsilon_b \beta \frac{A}{d_b} \left(\sigma_p \gamma \frac{A}{d_p} \right)^{-1} \\ &= (\varepsilon_0 \varepsilon_p / \sigma_p)(d_p/d_b)(\beta/\gamma) \end{aligned} \quad (15)$$

which lies between τ_1 and τ_2.

Electrically the system we have considered is indicated in Fig. 1a, with the cell properties in series with those of the barrier and both are scaled in terms of the effective measured conductance and capacitance. The measured capacitance for this circuit can be expressed in the form

$$C(\omega) = \frac{1}{i\omega} \left(\frac{1}{G_b + i\omega C_b} + \frac{1}{G_p + i\omega C_p} \right)^{-1} \quad (16)$$

This relationship can be displayed most easily on a log/log plot of the components of the complex capacitance

$$C(\omega) = C'(\omega) - iC''(\omega)$$

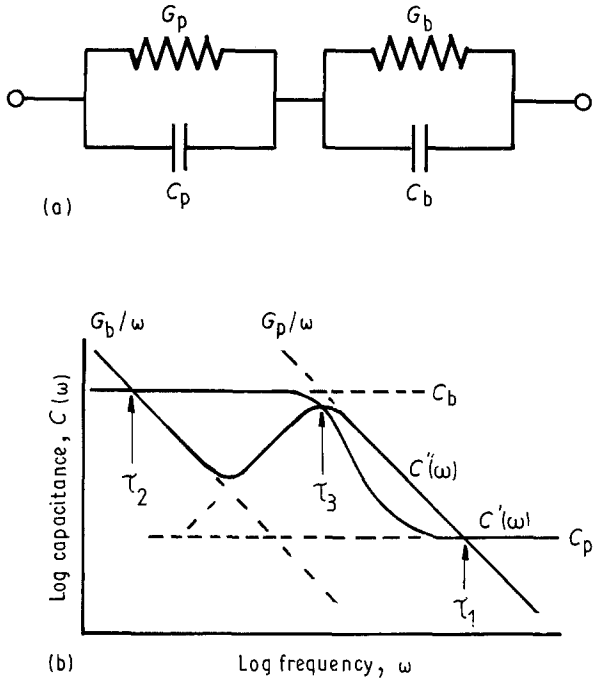

Figure 1 Schematic diagrams of (a) an elementary unit in an emulsion. G_p and C_p are the conductance and capacitance of a representation emulsion particle and G_b and C_b the conductance and capacitance of a single barrier between two particles; (b) representation in logarithmic coordinates of the complex capacitance resulting from the circuit in (a). τ_1, τ_2 and τ_3 are relaxation times as described in the text.

as functions of the frequency ω, as in Fig. 1b. The imaginary component, given by the conductances G, are shown, in the limiting conditions of high and low frequencies, as parallel lines with negative slope of unit magnitude ($C''(\omega) = G/\omega$) with $G_b \ll G_p$. The relaxation times τ_1, τ_2 and τ_3 are indicated in the figure.

Equation 16 can be developed in an analytical form, but for our purpose, Fig. 1b is a more useful method of presentation. From the figure we see that the frequency range required to observe the total response has to be in excess of

$$\begin{aligned} \tau_1/\tau_2 &= \varepsilon_p \sigma_b / \varepsilon_b \sigma_p \\ &= (\varepsilon_p/\varepsilon_b)(\sigma_b/\sigma_p) \end{aligned} \quad (17)$$

The magnitudes of the permittivities range from almost 80 for water to 2.5 for a typical hydrocarbon, giving a ratio of 32. The dominant term, however, is the ratio of the conductivities which can be of the order of 10^{10} or larger. Hence we require a frequency range of at least 10^8 in order to resolve both processes, without even extending into the outer wings of the τ_1 and τ_2 processes. Considering a particle of pure water at room temperature with a conductivity of 10^{-4} S the relaxation time, τ_1, is 10^{-5} s, equivalent to a frequency of 1.8×10^4 Hz so that it would be necessary to measure down to 10^{-4} Hz [14] in order to obtain the full spectrum of the response.

In the above paragraphs we have followed convention in assuming that the τ_3 relaxation process is a Maxwell–Wagner effect, in which the conduction within a particle is blocked by the capacitance associated with the walls of the same particle. As the components are in series, we have a well-defined relaxation

time, as shown in Fig. 1b, and hence the form of the relaxation is given by

$$C(\omega) = C_0 \frac{1 - i\omega\tau_3}{1 + (\omega\tau_3)^2} \quad (18)$$

In particular we note that for

$$\omega \to 0, C'(\omega) \to C_0 \quad \text{and} \quad C''(\omega) \propto \omega \quad (19)$$

and

$$\omega \to \infty, C'(\omega) \propto \omega^{-2} \text{ with } C''(\omega) \propto \omega^{-1} \quad (20)$$

which are the characteristic of the conventional Debye response [15].

As an example of the type of response that can be obtained, we show, in Fig. 2, experimental data for the complex capacitance as a function of frequency for a particular water-in-oil system. Two sets of data, measured at different temperatures, have been normalized together to give a single extended-frequency plot. In the figure the τ_3 relaxation lies in the region of the overlap in the data. The limiting behaviour of Relationships 19 and 20 are indicated by the dashed lines. It is clear that the experimental data do not fit these relationships. Indeed the only point of agreement is that the blocking capacitance, the capacitance of the barrier around the particles, is non-dispersive. A more general Maxwell–Wagner effect in which the barrier capacitance is dispersive has been reported [12, 16] but does not apply in this case either.

The alternative modification is to consider a non-dispersive barrier layer and an imperfect particle conductance, i.e.

$$G(\omega) = G_0(i\omega)^{1-s} \quad (21)$$

with $0 < s < 1$. Straightforward algebra gives the complex capacitance of the series connected capacitance and conductance as

$$C(\omega) = C_0[1 + (C_0/G_0)(i\omega)^s]^{-1} \quad (22)$$

from which we can derive the asymptotic frequency responses

$$\omega \to 0, C'(\omega) \to C_0 \quad \text{and}$$

$$C''(\omega) \to (C_0)^2(G_0)^{-1}\omega^s \sin(s\pi/2) \quad (23a)$$

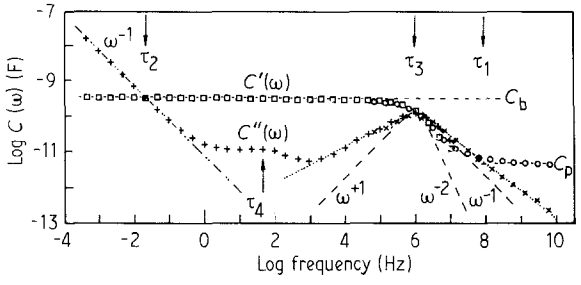

Figure 2 The complex capacitive response of a representative water-in-oil emulsion. These data were measured at 247 and 288.5 K and normalized to the single response curve. The dotted lines are the Debye characteristics of Equations 19 and 20, and the power-law relationships in the wings of the τ_3, are indicated by dashed lines. The characterization of this and other samples is given in Table I. The plot is scaled at 285 K.

and

$$\omega \to \infty, C'(\omega) \to G_0\omega^{-s}\cos(s\pi/2) \quad (23b)$$

$$C''(\omega) \to G_0\omega^{-s}\sin(s\pi/2) \quad (23c)$$

with the loss peak wings being of fractional power law form with frequency and symmetrical, on a log/log plot, about the peak loss frequency. This is the characteristic of the empirical Cole–Cole [17] dispersion function. From the data in Fig. 2 we estimate s from Equation 23c to be 0.76 and from Equation 23a to be 0.47, and hence the essential symmetry which is required for the Cole–Cole model has not been observed.

We conclude then, that the conventional approach for the interaction of particles within an array, which is obtained by extension of a simple Maxwell–Wagner response, does not correspond with the experimental situation which requires at least an additional parameter in order to describe the asymmetry of the experimentally observed response. In order to establish a reasonable framework within which it will be possible to consider an alternative approach it is essential to have detailed knowledge of the exact nature of the relaxation dispersions in water-in-oil emulsions. This we do in the present paper.

3. Experimental procedure

The data reported here were obtained with the aid of a Solartron frequency response analyser (FRA) configured with the Chelsea Dielectrics Interface. The measuring range was from 10 μHz to 10 MHz and care was taken in the design of the sample cells in order to minimize the effects of lead resistance. A single measurement at 10 μHz takes almost 2 days and, as the sample responses are temperature sensitive, the practical limitation on low-frequency measurements is the temperature stability of the sample cell. In practice most measurements were limited to the frequency range above 1 mHz. As the FRA uses a digitization technique there are truncation errors for very large or very small phase angles, with the error appearing as a random noise in the complex component of smaller magnitude. A sample cell using platinum electrodes of area 1.63×10^{-4} m^2 and capacitance 0.236 pF when empty was used during the larger part of the investigation. A measuring signal of 1 V r.m.s. amplitude was used after it had been checked that the response was linear with this value of voltage.

The emulsions were prepared using a planetary mixer with a primary orbital speed of 180 r.p.m. and a secondary orbital speed of 500 r.p.m. Over the range of samples the average droplet size was measured as about 2 μm. Two different surfactants were used in the investigation and these are referred to as surfactants A and B. Characterization of the samples reported here is presented in Table I, from which it can be seen that the series of samples were obtained by variation of the salt and water content whereas the total surfactant content was maintained at either 1.5% or 2%, by volume.

TABLE I Characterization of the samples reported in this paper. All samples were of the water-in-oil type with the water content being a mixture of saturated nitrate or chloride solution and pure water. The calcium nitrate was used in the form of calcium nitrate tetrahydrate

Sample no.	Measuring temp. (K)	Salt content		Water (%)	Oil (%)	Surfactant		Fig.
		Type	(%)			Type	(%)	
1	285.1, 244.7	Ammonium nitrate	47.5	0	3	A	2	2, 4c
		Calcium nitrate	47.5					
2[a]	329.4, freeze fracture	Ammonium nitrate	37.5	0	3	A	2	6, 7,
		Calcium nitrate	57.5					4a, b
3	296.3	Ammonium nitrate	78.7	16	3.8	A	1.3	5a
						B	0.2	
4	299.2, 326	Calcium chloride	40.0	54.5	4	A	0.75	5b, 8
						B	0.75	
5	296.5	Ammonium nitrate	56.8	37.9	3.8	A	0.5	6a
						B	1.0	
6(a)	297	Ammonium nitrate	71.0	23.7	3.8	A	1.5	6b

[a] A mixture of 47.5% calcium nitrate tetrahydrate and 10.0% anhydrous calcium nitrate was used.

4. Results

In Fig. 2 we have presented data measured on an ammonium nitrate/calcium nitrate/oil and emulsifier system at two temperatures. The plot has been scaled at 288.5 K and the data set measured at 244.7 K has had its frequency values multiplied by 1.3×10^4 in order to bring these data into alignment with those obtained at the higher temperature. Indicated in the plot are the values for the capacitances C_b and C_p and the loss associated with the conductances G_b and G_p, as described in Fig. 1. The data for Fig. 2 was obtained with an early cell for which the empty capacitance was 0.856 pF and hence, from Equation 5, ε_{eff} is 5.8 and ε_b is 440. The barrier conductance can be obtained from the low-frequency data as 5.6×10^{-11} S, and hence τ_2 is approximately 2×10^{-2} Hz^{-1}. An electron micrograph of this emulsion is shown in Fig. 3 and indicates a highly uniform particle size in the range 1–2 μm diameter. Taking the mean size as 1.5 μm and making use of the ratio of permittivities, we estimate the barrier thickness as of the order of 1 nm for the measured oil–surfactant mix permittivity of 2.5.

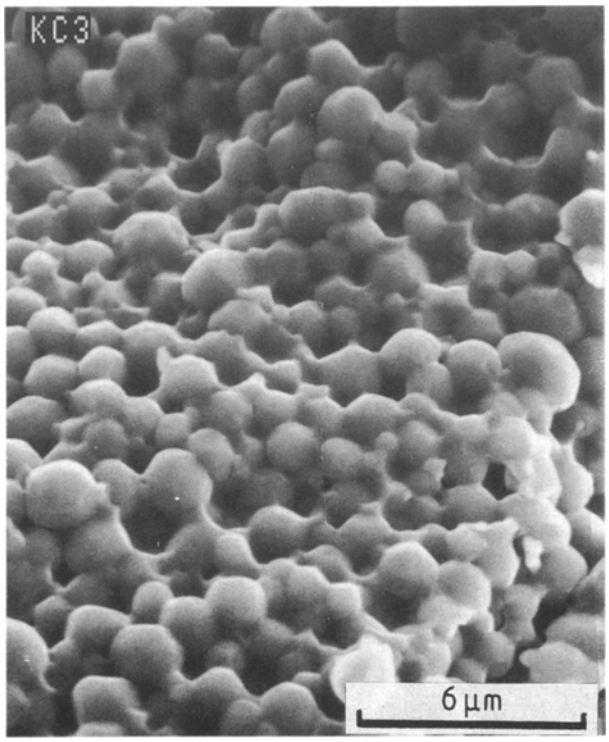

Figure 3 Freeze fracture scanning electron micrograph of Sample 2. 10 kV

The essential differences between the measured spectral response in Fig. 2 and the model equivalent of Fig. 1b are the poorly defined Maxwell–Wagner response with relaxation time τ_3 which has already been discussed, and an additional loss peak designated as τ_4 in Fig. 2. The evidence is that the capacitance associated with the τ_4 process is in parallel with the barrier conductance and hence is likely to be due to a dipolar content in the oil/emulsifier. In particular it is possible that the process could be associated with the pockets of oil/emulsifier formed between the corners of imperfectly matching particles. We shall return to consideration of this process in Section 4.3 after examination of the τ_3 response.

We note that in Fig. 2, even with some fourteen orders in magnitude of normalized frequency we have still not extended sufficiently into the high-frequency region to observe the solution dispersion. For water solutions this typically occurs in the region of 100 GHz at room temperature, some four orders of magnitude higher than that presented in the normalized plot. Measurements in this frequency range require sophisticated waveguide techniques.

4.1. The τ_1 and τ_2 relaxation processes

As defined in Equations 7 and 14 these are characteristic of parallel resistances and capacitances as can be seen in Fig. 2 for τ_2. As discussed in Section 4.2, a feature of the emulsion response is that the conductance, G_p, is dispersive so that the loss is not proportional to the inverse of the frequency. Nevertheless, Equation 10 allows us to define the relaxation time. As the capacitance C_p is non-dispersive the magnitude of the relaxation time is controlled by the loss associated with the τ_3 process.

4.2. The τ_3 relaxation process

The Debye nature of the Maxwell–Wagner relaxation process, cf. Equations 19 and 20, implies that the

process occurs without interaction between the relaxing elements [9, 10, 13]. Debye's original model for a rotating dipole [15] specifically considered that single dipoles were acted on by a common external field and restrained by a common macroscopic viscosity, so that the total response can be obtained by simple summation of the individual responses. It is now accepted that the broadening of loss peaks is due to some form of cooperative interaction and that the degree of broadening is a measure of the amount of this interaction [12, 18, 19]. A general cooperative relaxation model has been established by two of the authors [8, 9] and considers exactly the type of situation described here in which clusters (water particles) can relax internally in a cooperative manner but also hierarchically, so that the collection of particles relaxes cooperatively to give the total response of the assembly. In terms of this cluster model of relaxation, we can associate our particles with the elemental clusters and the exchange between clusters, which leads to the dynamic equilibrium of the assembly, as the equivalent of relaxation through the oil/emulsion barriers between the water particles. In the cluster model the total magnitude of the dispersion, $\chi(0)$, is a measure of the number of responding particles and the dipole moment associated with each. Hence we should not associate the increment $(C_b - C_{eff})$ in the capacitance with a simple barrier property as in the Maxwell–Wagner case.

An essential feature of the cluster model of relaxation is that fractional power-law dispersions are predicted, with the loss peak exhibiting an asymmetry in the general case, as observed in Fig. 2. In terms of the cluster model the higher frequency exponent, s ($= 0.76$), is equivalent to an efficiency for energy exchange within the particles of $1.0–0.76 = 0.24$ and the lower frequency exponent of 0.47 represents the efficiency of exchange between clusters. Unconstrained liquids normally have internal exchange efficiencies close to zero and high values of the inter-cluster exchanges that are close to unity [20] so we see that the effect of emulsification is to decrease the inter-particle exchanges whilst increasing the intra-particle exchanges.

In Fig. 4 we present the temperature dependence of the τ_3 loss peak as measured on two different samples, the compositions of which are given in Table I. The data were obtained in two of the cases on cooling the samples from room temperature, whereas the third sample, Sample a, was measured after cooling to 223 K and holding the emulsion at low temperatures, whereas for Run b, a different sample of the same material was cooled from room temperature and held at low temperatures whilst a set of measurements were made and then heated. It is clear from comparison of Fig. 4a and b that ageing takes place even when the sample is cool. It was for this reason that direct cooling of an as-prepared sample was used to obtain representative data. The data shown for Sample c were measured during its initial cooling run and shows the characteristic α-temperature dependence of a glass-forming system with the temperature at which the gradient of this plot becomes infinite being the glass

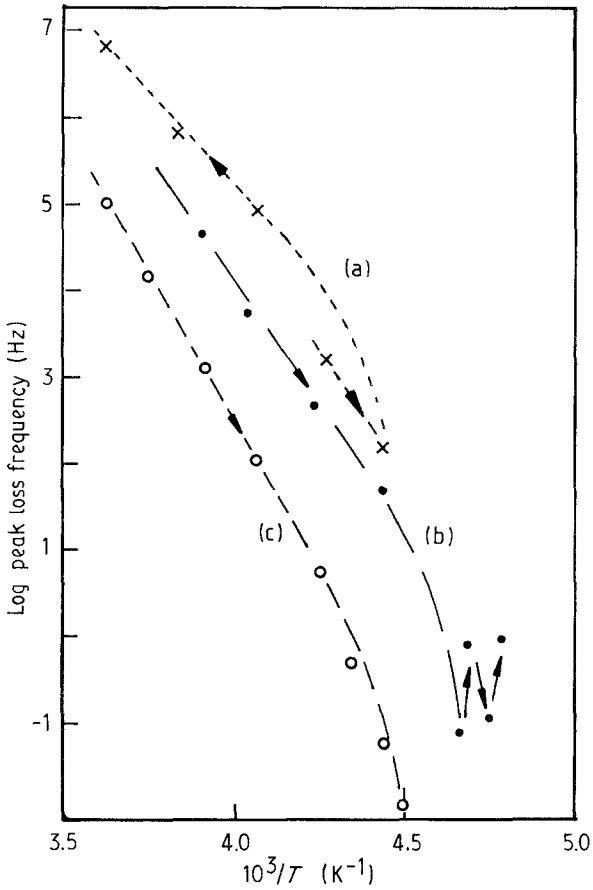

Figure 4 Arrhenius plot of the inverse of the τ_3 relaxation peak for (a, b) two samples of Mix 2 and (c) one of Mix 1.

transition temperature, T_g [21]. This set of data shows an activated process at high temperatures leading into the glass transition region with the glass transition temperature in the region of 218 K. It is known that the ammonium nitrate–calcium nitrate solution used for these samples forms a glassy solid and hence these data confirm that the τ_3 relaxation is associated with the solution within the particles of the emulsion.

4.3. The τ_4 relaxation process

In Fig. 2 we have labelled the additional loss peak in the region of 100 Hz the τ_4 relaxation, and noted that the process leading to this dispersion was in parallel with the barrier conductance. A range of different emulsion systems has been examined and the characteristics obtained in this dispersion region for all of these are shown in Figs 5 and 6.

Fig. 5a shows the response measured on a system of 94.7% nitrate and water solution, 3.8% oil and 1.5% surfactant. On changing the surfactant to a mixture of 1.3% of the original and 0.2% of the alternative the response shown in Fig. 5b was found. Fig. 6 shows a similar difference from a second pair of emulsions in which the differences are also in the surfactant and its volume fraction, as given in Table I. A common cell was used throughout these measurements so that a direct comparison can be made. It is clear that the presence (or absence) of the τ_4 feature depends on the emulsifier used. The lowest level of dispersion was observed with a mixture of emulsifiers, which may

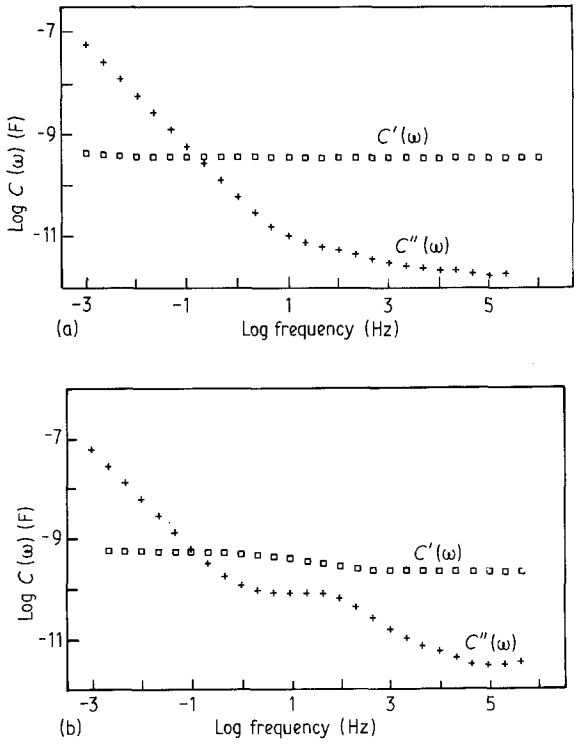

Figure 5 Capacitive dispersions for (a) Sample 3 and (b) Sample 4. Note the increase in loss, $C''(\omega)$, in the region of 30 Hz in (b) which we have labelled τ_4.

indicate local blocking of dipole motion by an interaction between the emulsifiers.

4.4. The d.c. conductance

The lowest frequency process that can be seen in Fig. 2 is that due to the d.c. conductance and which gives rise to the (parallel) relaxation τ_2. In Fig. 7 we present data measured at a high temperature (329.4 K) and over a frequency range down to 100 μHz. This has revealed a further dispersion in the capacitance but the loss continued to be dominated by the d.c. conductance. The power law behaviour shown by the discontinuous lines in the figure is that predicted for a true Maxwell–Wagner charge blocking process with the blocking barrier having a capacitance of the form

$$C(\omega) \propto (i\omega)^{-0.4} \qquad (24)$$

Such blocking layers have been observed with other emulsion systems and have been assigned to the formation of an oil–emulsifier blocking film on the surface of the electrodes of the cell [4, 10]. As the blocking film may be a monomolecular layer or a charge double layer, the barrier capacitance can be high. Examination of the low-frequency response in Fig. 7 indicates that the barrier capacitance will be in the region of 10^{-2} F which gives an effective barrier thickness of about 1.5×10^{-10} m even on taking the permittivity as that of water. We note that the characteristic $(i\omega)^{-0.5}$ can be obtained for a diffusive barrier layer and hence we postulate that the blocking layer observed here is somewhat diffusive in nature. There is no evidence that the transport of charge in the bulk of the emulsion is other than a perfect conductance although of small magnitude (1.4×10^{-10} S) and we consider that this weak conductance is due to impurities in the oil–emulsion layers and because of the diffusive nature it is likely to be due to ions.

This is not the case with the de-emulsified sample whose response is shown in Fig. 8. The lowest frequency process here is characterized by an anomalously large dispersion in both capacitance and loss with $C(\omega) \propto (i\omega)^{-p}$ and $p = 0.96_5$. The value of p has been determined to a high accuracy by making use of the relationship

$$C''(\omega)/C'(\omega) = \cot(p\pi/2) \qquad (25)$$

for in this case the ratio of the capacitances is large (and constant). In terms of the cluster model what was a perfect conductance before de-emulsification has now become an imperfect charge transport with an efficiency of transport of 0.965. The figure shows that de-emulsification has not removed the τ_4 relaxation process although the dominance of the electrode barrier layer has now weakened.

The magnitudes of the d.c. conductances for the samples whose characteristics are shown in Fig. 5a, b and 6b are identical and significantly different to that observed in Fig. 6a. All of these samples were measured at a temperature of 298.5 ± 2 K. Examination of Table I shows that it is unlikely that the difference is due to the solution, whereas a pattern can be seen in terms of the surfactant mix. In Fig. 9 we plot the

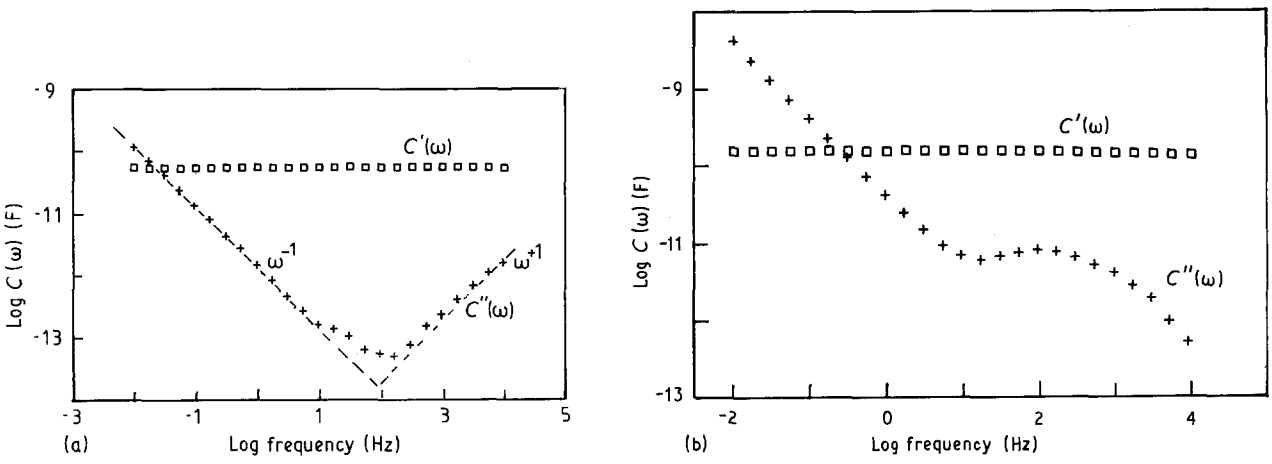

Figure 6 Capacitive dispersions for (a) Sample 5 and (b) Sample 6. Both of these samples are based on ammonium nitrate solutions but again there is a significant difference in the τ_4 process.

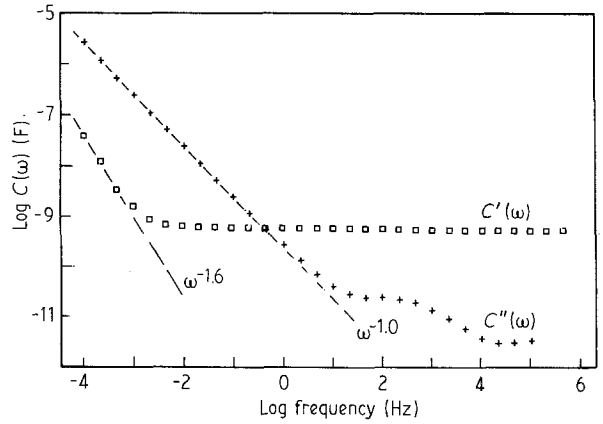

Figure 7 A measurement on Sample 2 at high temperatures. At low frequencies the response is dominated by a d.c. conductance which is truncated by a power-law response barrier layer giving the non-Maxwell–Wagner dispersion in the capacitance.

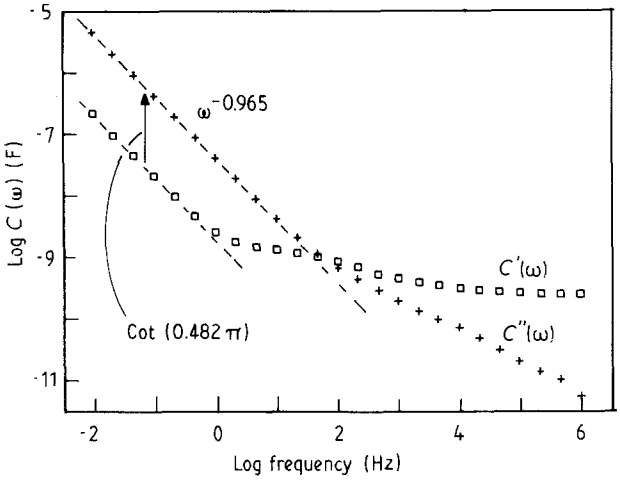

Figure 8 A measurement on Sample 8 after de-emulsification had taken place. As for the previous figure, this measurement was made at a high temperature and the results can be compared. Physically the structure of this sample was disordered.

values of the d.c. conductance as a function of the concentration of surfactant A at a constant surfactant concentration of 1.5%. It is clear that the d.c. conductance is sensitive to the nature of the surfactant and that the bulk conductance decreases when A forms less than one-third of the total. In the same figure we also give the constant capacitance, C_b, which we observe is also a function of the surfactant mix. In terms of the simple model outlined in Section 1 we can relate C_b to the inverse of the thickness of the barrier layers so that we might expect a high capacitance (thin barrier) to be associated with a high conductance if the conductance is basically a leakage from cell to cell or else with a low conductance if the conductance paths are through the inter-particle barriers. It is clear that the latter is not the case here and our d.c. conductance is basically a leakage current and sensitive to the thickness of the barriers.

5. Discussion

In our analysis of the experimental situation, we have made use of the simplest electrical model of an emul-

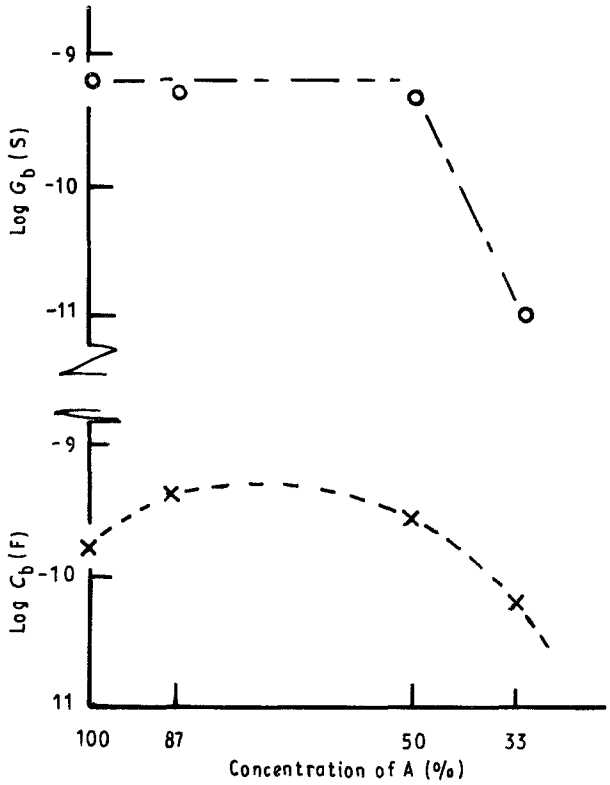

Figure 9 Logarithmic plots of the low-frequency conductance and the capacitance, C_b, as functions of the concentration of A in the surfactant mix.

sion structure. There are two reasons for doing so. Firstly this allows us to concentrate on the physical construction of the emulsion. We have also investigated a more complicated approach in which we took a reasonable model of the particles, that is their size and shape, emulsion/oil barrier thickness, and cell geometry as our elements. This resulted in a response characteristic identical to that presented in Fig. 1b so it gave no additional information about the form of the response than the simple model used here. A second alternative was to use the Hanai [6, 7] model which requires solution of a third-order equation [22]. Having constructed suitable computer programs to do this, it was observed that the response plots, as a function of frequency over a reasonable range of variables, were again of the form of Fig. 1b. A detailed examination of the Hanai function has been carried out and the results of these calculations are reported in Table II. A standard water-in-oil emulsion has been considered and the forms of the spectral response and the magnitudes of its characteristic parameters are reported. We have termed the high volume fraction dispersions as being of the Cole–Davidson form but the high-frequency side of the loss peak exhibited continuous curvature from the peak loss out over two or three magnitudes of frequency before the Debye gradient was obtained.

Examination of the Hanai approach shows an invalid assumption in the development of the model from low volume fractions, $< 30\%$, to high volume fractions. The assumption makes use of the volume fraction as the variable of integration in order to model, in some way, the cooperative effects that set in

TABLE II Characterization of the Hanai model of cooperative dispersion as determined from Clausse and Royer's description [24]: $\varepsilon_1 = 80.4$, $\sigma_1 = 10^{-3}$, $\varepsilon_2 = 2.5$, $\sigma_2 = 0$ (water-in-oil)

Vol. fract.	Form of dispersion	Parameterization[a]		
		$\Delta\varepsilon$	ε_∞	ω_p (Hz)
0.05	Debye	0.042	2.874	9×10^4
0.10	Debye	0.107	3.322	8×10^4
0.20	Debye	0.368	4.513	7×10^4
0.40	Debye	2.63	8.94	5×10^4
0.50	Cole–Cole, $\alpha = 0.025$	7.05	12.95	4×10^4
0.60	Cole–Cole, $\alpha = 0.045$	19.08	19.1	3×10^4
0.70	Cole–Cole, $\alpha = 0.07$	69.7	28.4	1.7×10^4
0.80	Cole–Cole, $\alpha = 0.13$	346	38.7	6×10^3
0.85	Cole–Davidson[b]	692	48.9	5×10^3
0.90	Cole–Davidson[b]	2.4×10^3	58.2	10^3
0.95	Cole–Davidson[b]	2×10^4	58.6	10^2
0.975	Cole–Davidson[b]	1.6×10^5	74.4	20

[a] $\Delta\varepsilon$ is the magnitude of the dispersion in the permittivity; ε_∞ is the "infinite" frequency permittivity, and ω_p is the frequency of the maximum in the loss.

[b] Note that the process referred to here as Cole–Davidson is poorly defined in that there is no region with a well-defined power-law characteristic for $\omega > \omega_p$ but a region of continuous curvature from the peak loss to ω^{-1} over two or three orders of magnitude in frequency.

for the higher volume fractions. There was no evidence from the calculations that in fact this had been done.

We have shown, from examination of the dispersion characteristics of a range of emulsions, a number of general features. There is broad agreement with a simple model of a particle which is electrically in series with its surface barrier. Within the accessible frequency range no information was available about the nature of the dispersion in the liquid itself but the temperature dependence of the τ_3 relaxation shows clearly, in this investigation at least, that it is the salt solutions that are contained in the particles. The effective thickness of the barriers around the particles can be determined from Equation 12, corrected for the numbers of layers of particles in the emulsion sample. This gives d_b for a single layer as 0.12 nm whereas extrapolation to the Maxwell–Wagner barrier in Fig. 7 suggests a single barrier thickness of an order of magnitude less.

The most important feature reported here is the form of the dispersion of the τ_3 loss peak. We have shown that it is neither a Debye, a Cole–Cole, nor a Cole–Davidson dispersion, nor of the distorted Cole–Davidson form observed from the Hanai function.

At very low frequencies, two types of dispersion have been observed. For a de-emulsified sample the imperfect charge transport in the disordered structure leads to an equivalent dispersion in the capacitance and a constant phase response for the system. In the ordered emulsion a conductance, characterized by a perfect inverse frequency dependence of the dielectric loss, in parallel with a power-law dispersion in the capacitance, has been observed. It has been deduced that the capacitance dispersion is due to a Maxwell–Wagner charge blocking by a barrier layer which is itself dispersive due to space charge build up at the electrodes and a diffusive transport of the carriers in this region.

One new relaxation process has been found and examined. In the frequency range lying between the τ_3 and τ_2 loss peaks, an additional process has been observed and related to the surfactants used to form the emulsions. In particular it was noted that a mixture of surfactants reduced the effect of this loss process and hence it is less likely that it is due to impurities in the surfactants than to an inherent property within the mix of surfactants.

6. Conclusions

The present investigation of the dielectric responses of a range of emulsion systems has shown the need for careful experimental examination of specific systems in order to carry out critical evaluations of each of the individual features that have been delineated. It is clear from the work reported here that the cooperative nature of the system can best be observed in the τ_3 response. At higher frequencies than those reported here the response will be dominated by the water or solution, and hence the frequency region of interest lies below about ~ 10 MHz. At frequencies in the microhertz range the response is dominated by charge transport within the bulk of the sample which gives useful information about the long-range order. The frequency range in which useful information about the nature of the cooperative effects of the emulsion, which gives it its stability, can be obtained between the millihertz and megahertz range, the region of the τ_3 and τ_4 dispersion processes.

Acknowledgement

The authors acknowledge the assistance given to them in programming the Hanai function by Ms E. S. Beckford.

References

1. C. ROBERTUS, J. G. H. JOOSTEN and Y. K. LEVINE, *Phys. Rev. A.* **42** (1990) 4820.
2. M. CLAUSSE, "Dielectric Properties of Emulsions and Related Systems", in "Encyclopedia of Emulsion Technology",

Vol. 1, edited by P. Becker (Dekker, New York, 1983) pp. 481–715.
3. L. A. DISSADO, R. C. ROWE, A. HAIDAR and R. M. HILL, *J. Coll. Interface. Sci.* **117** (1987) 310.
4. R. C. ROWE, L. A. DISSADO, S. H. SHAIDI and R. M. HILL, *ibid.* **122** (1988) 354.
5. L. K. H. VAN BEEK, "Progress in Dielectrics", Vol. 7, edited by J. B. Birks (Heywood Press, London, 1967).
6. T. HANAI, *Kolloid Z.* **171** (1960) 23.
7. *Idem, ibid.* **175** (1961) 61.
8. L. A. DISSADO and R. M. HILL, *Proc. Roy. Soc.* **A390** (1983) 131.
9. *Idem, J. Appl. Phys.* **66** (1989) 2511.
10. R. M. HILL, E. S. BECKFORD, R. C. ROWE, C. B. JONES and C. A. DISSADO, *J. Coll. Interface Sci.* **138** (1990) 521.
11. R. M. HILL, *Nature* **275** (1978) 96.
12. A. K. JONSCHER, "Dielectric Relaxation in Solids" (Chelsea Dielectrics Press, London, 1983).
13. K. J. LISSANT, *J. Coll. Interface Sci.* **22** (1966) 462.
14. R. M. HILL, L. A. DISSADO, J. PUGH, M. G. BROADHURST, C. K. CHIANG and K. J. WALLESTRAND, *J. Biol. Phys.* **14** (1986) 133.
15. P. DEBYE, "Polar Molecules" (Dover Press, New York, 1945).
16. R. M. HILL and C. PICKUP, *J. Mater. Sci.* **20** (1985) 4431.
17. K. S. COLE and R. H. COLE, *J. Chem. Phys.* **9** (1941) 341.
18. R. G. PALMER, D. L. STEIN, E. M. ABRAHAMS and P. W. ANDERSON, *Phys. Rev. Lett.* **53** (1984) 958.
19. R. M. HILL and A. K. JONSCHER, *Contemp. Phys.* **24** (1983) 75.
20. J. ALISON, PhD thesis, London University (1991).
21. R. M. HILL and L. A. DISSADO, *J. Phys. C. Solid State Phys.* **15** (1982) 5171.
22. M. CLAUSSE and R. ROYER, *J. Coll. Interface Sci.* **2** (1976) 217.

Received 6 November
and accepted 2 December 1991